Journal of Solid State Electrochemistry (2019) 23:565–572
https://doi.org/10.1007/s10008-018-4163-0

ORIGINAL PAPER

TiO_2 nanoparticles anchored on three-dimensionally ordered macro/mesoporous carbon matrix as polysulfides' immobilizers for high performance lithium/sulfur batteries

Chunyong Liang[1] · Xiaomin Zhang[1] · Yan Zhao[1] · Taizhe Tan[2] · Yongguang Zhang[1]

Received: 28 July 2018 / Revised: 20 November 2018 / Accepted: 22 November 2018 / Published online: 4 December 2018

Abstract

A three-dimensionally (3D) ordered macro/mesoporous carbon (3DOMC) is synthesized by one-step template method as a TiO_2 supporter, and this TiO_2/3DOMC hybrid plays the role of immobilizers and can limit any polysulfides from escaping the cathode. The TiO_2/3DOMC exhibits high pore volume and specific surface area, accommodating up to 73.2 wt% in sulfur content. As a sulfur host, S/TiO_2/3DOMC composite was able to delivered 1105 mAh g^{-1} on first discharge and 695 mAh g^{-1} after 150 cycles at a current rate of 0.5 C. Even though at 2 C this material was able to keep a capacity of 551 mAh g^{-1}. We attribute the superior performance to the good conductivity and structural restriction of carbon and the intense electrostatic attraction between metal-oxygen bond and polysulfides to encapsulate sulfur of the TiO_2/3DOMC.

Keywords Lithium ion battery · Three-dimensionally (3D) ordered macroporous carbon (3DOMC) · TiO_2/3DOMC hybrid · Good conductivity · Intense electrostatic attraction

Introduction

Lithium/sulfur (Li/S) batteries have attracted great research interest in these years because of its high theoretical capacity of 1672 mAh g^{-1} and corresponding, energy density of 2600 Wh kg^{-1} [1–5]. Moreover, the natural abundancy and low toxicity of sulfur makes it a prospective cathode for rechargeable lithium batteries [6–8].

Unfortunately, Li/S batteries suffer from severe performance drawbacks that limits any potential applications. This is due to many problems, such as low electronic conductivity of sulfur, dissolution of high-order polysulfides, and volume expansion of sulfur to lithium sulfide [9].

✉ Yan Zhao
yanzhao1984@hebut.edu.cn

✉ Yongguang Zhang
yongguangzhang@hebut.edu.cn

[1] School of Materials Science and Engineering, Research Institute for Energy Equipment Materials, Hebei University of Technology, Tianjin 300130, China

[2] Synergy Innovation Institute of GDUT, Heyuan, Guangdong Province, China

Numerous attempts have been made to overcome such disadvantages mentioned above, including the compositing sulfur with carbon or conductive polymer matrix, reformulation of electrolyte and porous oxide additives [10–14]. The first-row transition metal sulfides are selected as the model system to obtain a general principle for the rational design of sulfur cathode and the strong adsorption that is induced by charge transfer between transition metal atoms and S atoms in Li_2S is confirmed to be of great significance in the composite cathodes [15]. Such as CoS_2 [16], TiO_2 [17] as well as Ti_nO_{2n-1} [18] have attracted great attention. TiO_2 with its polysulfide adsorbing ability and its low cost is considered as a particularly promising candidate. Li et al. prepared mesoporous TiO_2 spheres with large pore volume, serving as a stable reservoir to act as a mass sink for polysulfide species, and the S/TiO_2 composites exhibit good electrochemical properties, realizing an initial discharge capacity of 909 mAh g^{-1} with 705 mAh g^{-1} after 100 cycles [19]. In Tao et al.'s study, the superior properties of Ti_4O_7-S are attributed to the strong adsorption of sulfur species on the low-coordinated Ti sites of Ti_4O_7 as revealed by density functional theory calculations and confirmed through experimental characterizations [18]. However, the conductivity of TiO_2 is generally low, which severely limited the sulfur utilization and rate capability.

In the previous study, it has been well proven that the carbon with ordered interconnected macro/mesoporous network structure possesses excellent electrical conductivity and mechanical stability. Many inorganic-/nanocarbon-based sulfur host materials have been applied to lithium-sulfur batteries by researchers and have achieved good results. Chen's group did a lot of research on cobalt and cobalt sulfide embedded in carbon material, including "sea urchin"-like cobalt nanoparticle embedded and nitrogen-doped carbon nanotube/nanopolyhedra (Co-NCNT/NP) superstructures [20], metallic and polar Co_9S_8 nanocrystals inlaid carbon (Co_9S_8/C) hollow nanopolyhedra [21], interconnected carbon nanotubes inserted/wired hollow Co_3S_4 nanoboxes (CNTs/Co_3S_4-NBs) [22], carbon nanotubes reinforced CoS nanostraws (CNTs/CoS-NSs) [23], and cerium oxide (CeO_2) nanocrystals homogeneously into well-designed bimodal micromesoporous nitrogen-rich carbon (CeO_2/MMNC) [24]. Herein, we first demonstrate the synthesis of 3D ordered macroporous carbon (3DOMC) by one-step template method as a TiO_2 supporter for application in lithium sulfur battery. This TiO_2/3DOMC hybrid plays the role of polysulfide immobilizers that can effectively limit the diffusion of polysulfides away from the cathode. Meanwhile, 3DOMC could offer a continuous electron/Li^+ pathway to guarantee electrical contact, and allow for efficiency electrolyte uptake into the composite.

Experimental section

Preparation of 3DOMC

Monodisperse silica spheres were synthesized by hydrolysis of TEOS an ammonia solution, which was then centrifuged and dispersed in ethanol. When the ethanol solution evaporated completely, the silica opal was formed and would be used as a template. The 3DOMC was prepared by using resol as a carbon source via carbonization of the precursor and the silica opal template was removed with HF solution.

Deposition of TiO_2 on 3DOMC

The TiO_2 presoma solution was prepared by sol-gel, in a typical preparation of TiO_2 presoma solution was first sealing agitated the hydrochloric acid, tetraisopropyl titanate (TTIP) and ethyl alcohol were added, then the mixture was magnetic stirred for 1.5 h to form clear gel. Immersed the 3DOMC template in the TiO_2 presoma solution for a day, get out of the template and there will be TiO_2 presoma solution on top of it, 3DOMC with TiO_2 deposited was collected by stewing for 3 days and heated at 450 °C for 1 h at nitrogen atmosphere for further use.

Preparation of S/TiO_2/3DOMC composite

Nano sulfur and the as-prepared TiO_2/3DOMC with a weight ratio of 3:1 were mixed heated to 155 °C for 10 h in an enclosed container under a nitrogen atmosphere with the heating rate of 5 °C min^{-1}. The S/TiO_2/3DOMC composite is a composite cathode material of S and TiO_2/3DOMC prepared by sol-gel method loading titanium dioxide on a 3DOMC substrate and then hydrothermally reacting with sulfur (Fig. 1).

Characterization

The physiochemical properties of TiO_2/3DOMC and S/TiO_2/3DOMC composite were examined by various techniques. The surface morphology and elemental composition of the materials were obtained from a scanning electron microscopy (SEM, S-4800, Hitachi Limited), which equipped with EDX elemental analysis, and the TEM studies were obtained from a transmission electron microscopy (TEM, Jeol-JEM-2100F). The crystal structure and phase of the samples were studied

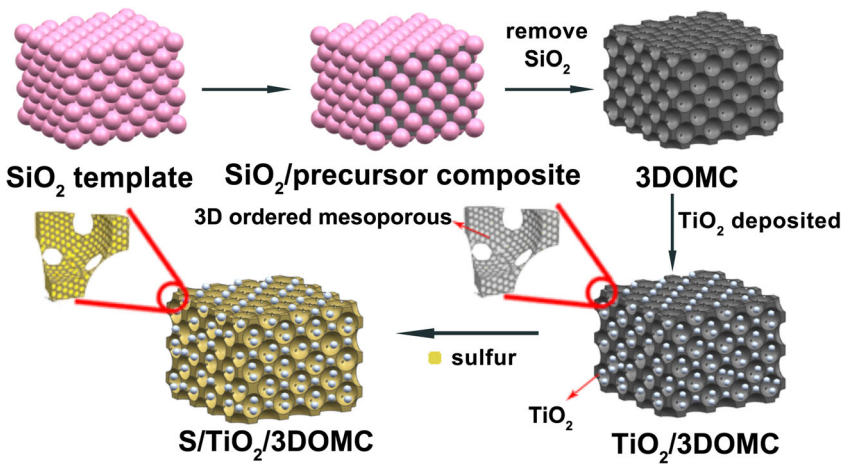

Fig. 1 Schematic of the preparation of the S/TiO_2/3DOMC

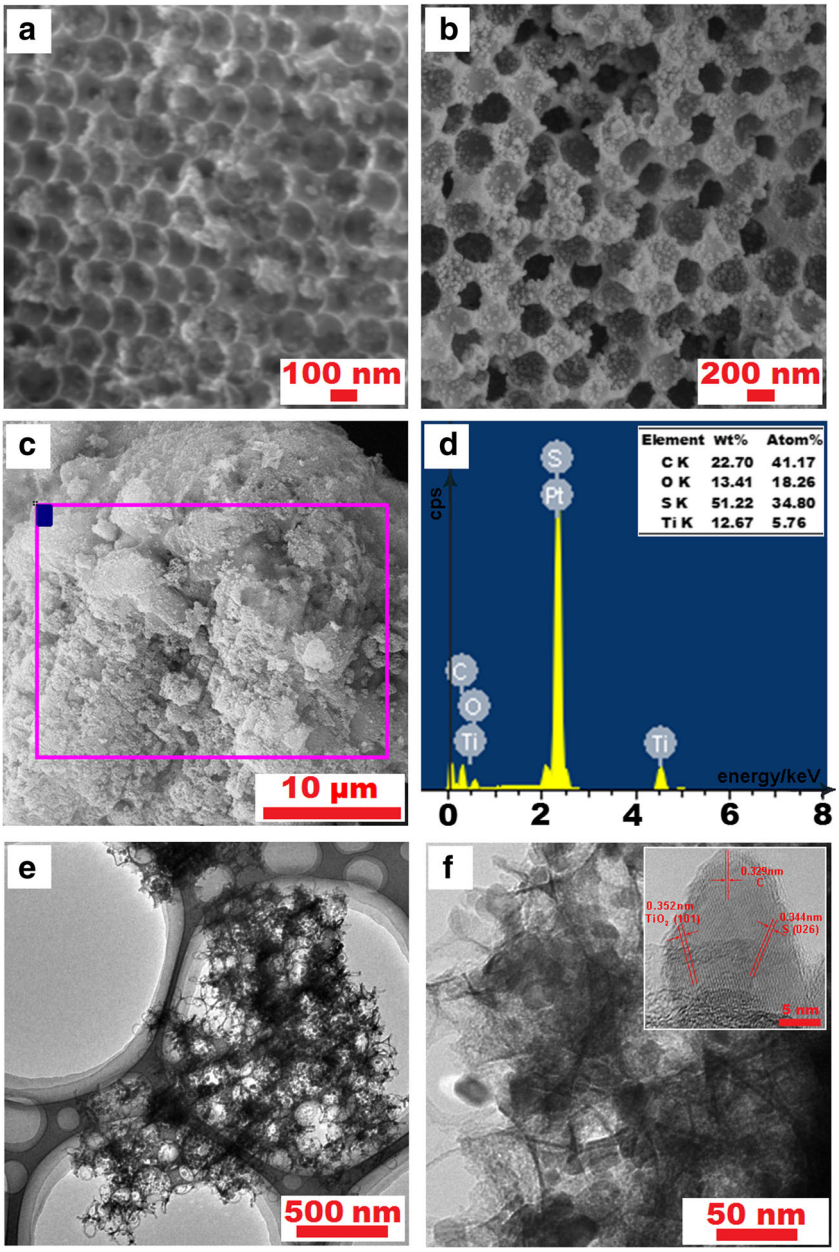

Fig. 2 SEM images of **a** the TiO_2/3DOMC composite; **b**, **c** the S/TiO_2/3DOMC composite; **d** the EDS analysis for the S/TiO_2/3DOMC composite; **e**, **f** TEM images of the S/TiO_2/3DOMC composite; inset: HRTEM image of the S/TiO_2/3DOMC composite

by X-ray diffraction (XRD, Rigaku-TTRIII, Tokyo, Japan) with Cu K_α radiation. The XPS spectrum was measured with an X-ray photoelectron spectroscopy (XPS, VG ESCALAB MK II, VG Scientific, Princeton, NJ, USA). The sulfur loading content was estimated by thermo gravimetric analysis (TGA, SDTQ600) under argon. The nitrogen adsorption-desorption isotherms were detected by Brunauer-Emmett-Teller (BET, ASAP 2020, Micromeritics, Norcross, GA, USA).

Electrode preparation and electrochemical measurements

The working electrode was prepared by grinding the mixture of S/TiO_2/3DOMC composite, Super P and poly-(vinyl difluoride) (PVDF) at a weight ratio of 8:1:1 dissolved in 1-methyl-2-pyrrolidinone (NMP) and the slurry was evenly coated on a carbon-containing aluminum foil, then the electrode was cut into pellets with a diameter of 1.5 cm after drying at 60 °C for 12 h. 2025-type stainless steel coin cells were assembled for testing the electrochemical performance, the assembly process was in an Ar-filled glove box. The prepared S/TiO_2/3DOMC composite work electrode was used as a positive electrode and the negative electrode material was a lithium metal sheet with a same diameter. The electrolyte was 1.0 M lithium bis (trifluoromethanesulfonyl) imide (LiTFSI) in 1,3-dioxolane (DOL) and 1,2-dimethoxyethane (DME) (1:1 by volume) with 1.0 wt% $LiNO_3$ additive. Galvanostatic charge/discharge measurements were carried

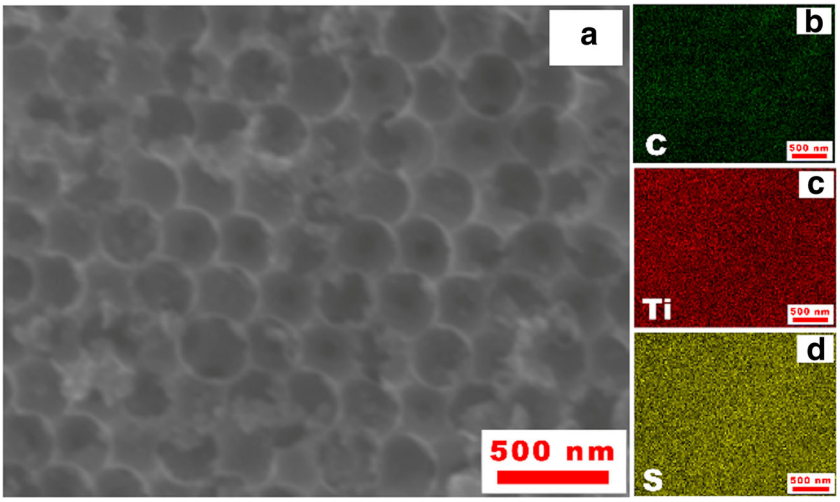

Fig. 3 **a** SEM image of the S/TiO_2/3DOMC composite; the elemental mapping images of **b** C, **c** Ti, and **d** S

out on a multichannel battery tester (BTS-5 V 5 mA, Neware), the applied currents and specific capacities were calculated on the basis of the weight of sulfur in the cathode. The cyclic voltammogram (CV) measurements was conducted by a PARSTAT 4000 electrochemical workstation, and the CV curves were measured from 1.5 to 3.0 V at a scanning rate of 0.1 mV S^{-1}. All of the electrochemical measurements were measured at room temperature. The mass loading of sulfur was around 0.4 mg cm^{-2}. In the process of preparing the battery, about 30 μL of electrolyte were added to each battery.

Results and discussion

As shown in Fig. 2a, there are obvious three-dimensionally ordered macro/mesoporous structure in the TiO_2/3DOMC composite, and the carbon porous network was coated with TiO_2 nanoparticles. This network structure of the porous carbon coated with TiO_2 nanoparticles lead to a high specific surface area (SSA). As revealed in Fig. 2b, the SEM image clearly show that the S/TiO_2/3DOMC composite still preserve a porous network structure. Figure 2c shows SEM image of S/TiO_2/3DOMC composite of different magnification. Furthermore, the corresponding EDS analysis was shown in Fig. 2d, the energy spectrum of the elements C, Ti, O, and S in the sample displayed that a good combination of sulfur and the matrix, and the elemental mapping images and the graphs (Fig. 3) provides a further evidence for this statement, which intuitively shows the uniform distribution of C, Ti, and S elements in the composite. High-resolution TEM (HRTEM) (Fig. 2e) shows the S/TiO_2/3DOMC composite have pores with a diameter of 150 nm. This porous network structure supply high SSA to ensure high contact area with electrolyte for efficient polysulfide adsorption. The lattice fringes of TiO_2, S, and C can be clearly noticed in Fig. 2f, suggesting a well-defined crystal structure.

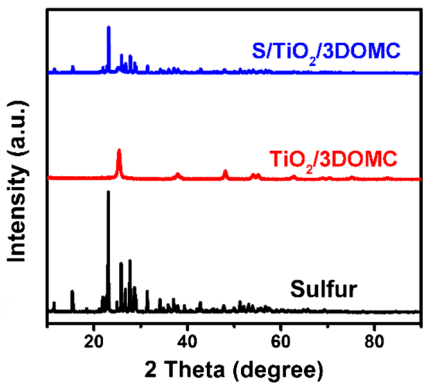

Fig. 4 XRD patterns of the sulfur, TiO_2/3DOMC matrix, and S/TiO_2/3DOMC composite materials

The XRD pattern (Fig. 4) of TiO_2/3DOMC reveals a broad peak at about $2\theta = 26°$ which is also found in the S/TiO_2/3DOMC composite sample. This peak corresponding to a certain degree of graphitized carbon, demonstrating that the TiO_2 and sulfur both have achieved a good combination with the three-dimensionally ordered macro/mesoporous carbon framework. Furthermore, the intensity of sulfur in the S/TiO_2/3DOMC composite is significantly weaker than that of its own diffraction peak, indicating that sulfur was well-dispersed in the pores of TiO_2/3DOMC matrix.

The chemical states of the S/TiO_2/3DOMC nanohybrid are determined by X-ray photoelectron spectroscopy (XPS, Fig. 5). Figure 5a presents the survey spectrum of S/TiO_2/3DOMC composite, which contains O, Ti, C, and S elements. As shown in Fig. 5b, the S 2p 3/2 peak at 164.1 eV and S 2p 1/2 peak at 163.7 eV 1:2 ratio which is typical of sulfur in composite. The S-O peak was at 164.4 eV. And the broad peak between 168 and 171 eV can be considered as sulfate species. The high-resolution spectrum of Ti 2p exhibits two main peaks at 459.9 eV and 465.5 eV can be attributed to the core levels of Ti 2p 3/2 and Ti 2p 1/2 in Fig. 5c. The C1s (Fig. 5d)

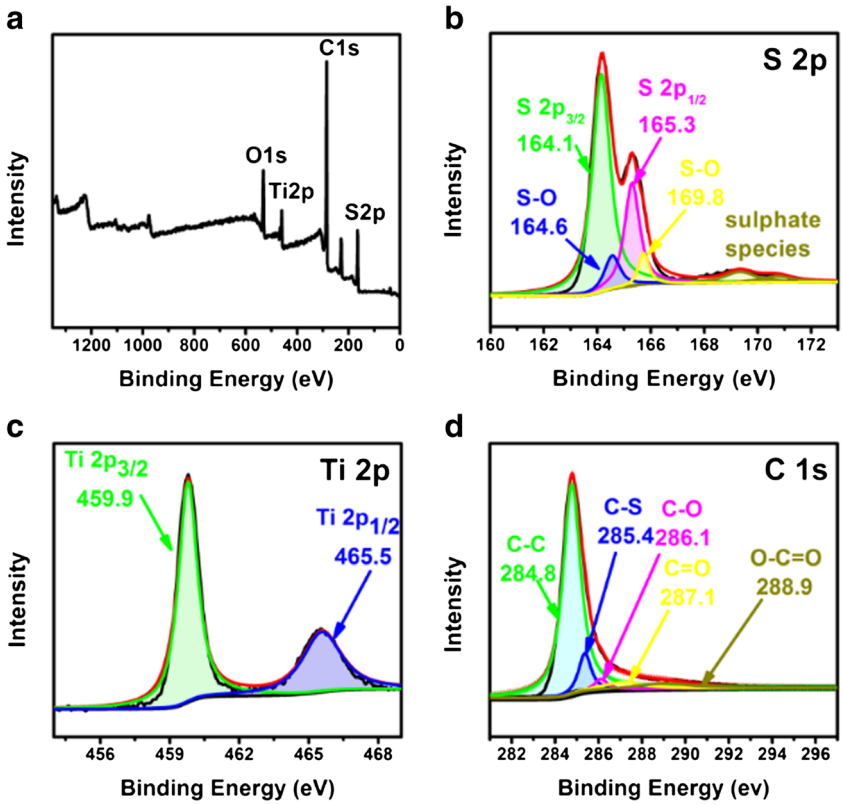

Fig. 5 **a** XPS survey scan, **b** S 2p, **c** Ti 2p, and **d** C 1s of S/TiO $_2$/3DOMC composite sample

spectra exhibits characteristic binding energies at about 284.8, 285.4, 286.1, 287.1, and 288.9 eV, which corresponding to C–C, C–S, C–O, and O–C=O, respectively. The existence of these chemical bonds further proves the good combination of the elements in the S/TiO_2/3DOMC composite and provides support for its good electrochemical properties.

From the N_2 sorption isotherms of TiO_2/3DOMC, a type IV (mesoporous nature) sorption behavior in the N_2 adsorption-desorption isotherms. Theoretically, the N_2 adsorption-desorption isotherm is more accurate for measuring the porosity characteristics less than 100 nm. In our work, the pore size of the 3DMOC matrix is about 150 nm. These pores are actually interconnected with each other in 3DMOC. We found that the resulting material is also rich in mesopores, which is confirmed by the type IV curve in the adsorption-desorption analysis. As we have seen, the pore-size-distribution of TiO_2/3DOMC host reveals pores of 10–20 nm in diameter, it was confirmed that the mesoporous structure exists in the sample (the pore volume represents the result of dV/dlogD). According to inference, the porous structure of this diameter is formed by stacking a large number of pores. In alignment with the previous HRTEM and SEM results, there also are a certain number of macropores with the diameter of about 150 nm. The sorption hysteresis of TiO_2/3DOMC is larger than that of S/TiO_2/3DOMC composite, suggesting that a larger portion of volume is represent by mesopores in TiO_2/3DOMC. The mesoporous structure allowed for a relatively high SSA of 188.94 $m^2\ g^{-1}$ and a pore volume of 21.05 $cm^3\ g^{-1}$. After being combined and

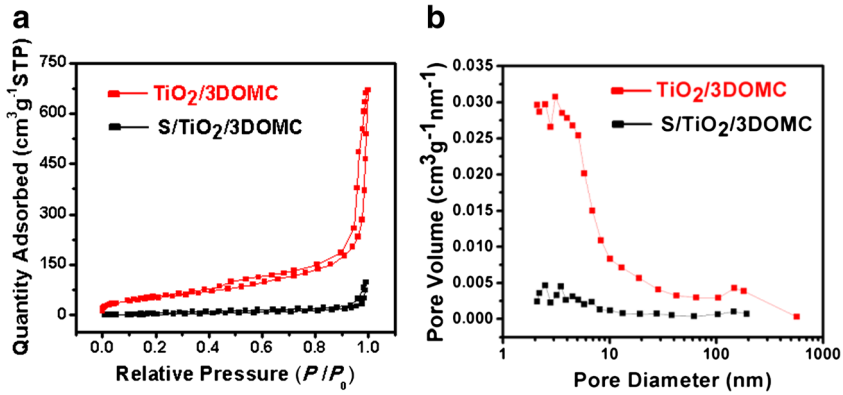

Fig. 6 **a** N_2 adsorption–desorption isotherms and **b** corresponding pore-size-distribution of TiO_2/3DOMC and S/TiO_2/3DOMC composite

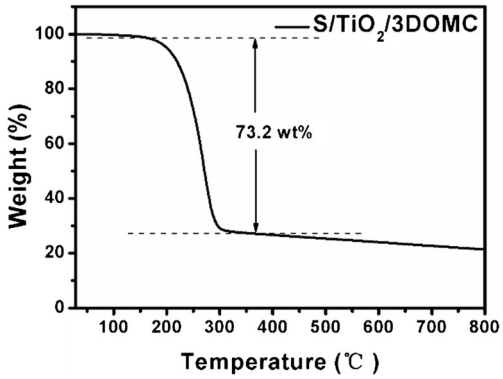

Fig. 7 TGA curves of S/TiO_2/3DOMC composites in N_2

heated with sulfur, the S/TiO_2/3DOMC composite exhibits the smallest SSA (28.60 m^2 g^{-1}) and pore volume (1.04 cm^3 g^{-1}), suggesting a successful infiltration of sulfur into pores of the TiO_2/3DOMC composite (Fig. 6).

As shown in the thermogravimetric analysis data (Fig. 7), the sulfur contents of S/TiO_2/3DOMC composite was around 73.2%. The minor weight loss in TGA curves of the S/TiO_2/3DOMC composite at a temperature from 180 to 350 °C, which could owing to the residual adsorbed water molecules and the evaporation of sulfur. This sulfur content is not much different from the mass ratio of sulfur mixed into the experimental operation, reflecting the strong current carrying capacity of the TiO_2/3DOMC matrix structure. The high sulfur content in our composites will offer a more practically viable absolute energy density.

To analyze the electrochemical behavior of the S/TiO_2/3DOMC electrodes, cyclic voltammetry (CV) at 0.1 mV s^{-1} of the first three cycles were collected with the voltage from 1.5 to 3.0 V, as shown in Fig. 8a. It can be seen that there are two pronounced peaks appearing at near 2.25 V and 2.0 V during the reduction process. The peak at 2.25 V can be related to the reduction of elemental S to soluble lithium polysulfide whereas

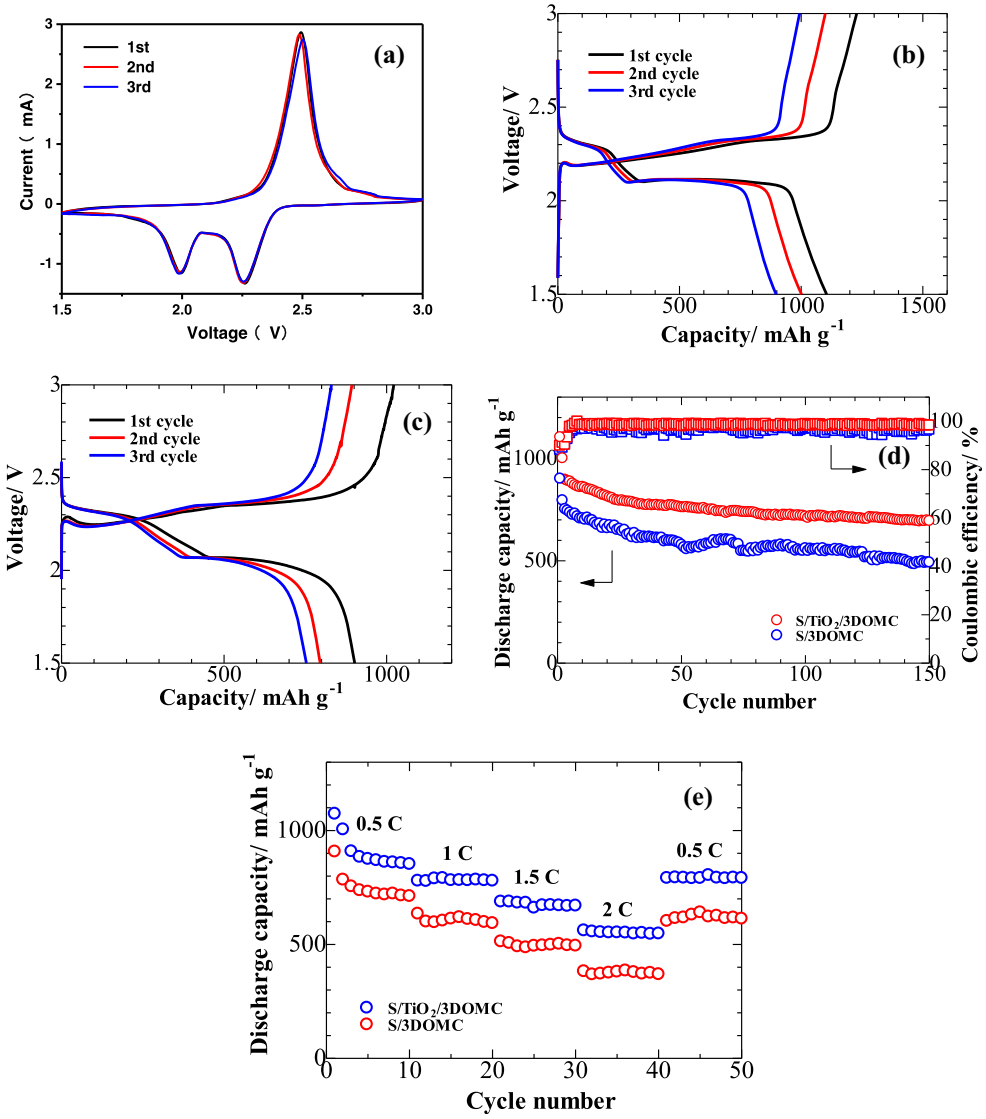

Fig. 8 **a** CV curves of a S/TiO_2/3DOMC/Li cell at a sweep rate of 0.1 mV S^{-1}, Discharge/charge performance of a **b** S/TiO_2/3DOMC/Li cell and **c** S/3DOMC/Li cell at 25 °C at 0.5 C between 1.5 and 3 V, **d** cycling performance and coulombic efficiency of S/TiO_2/3DOMC/Li and S/3DOMC/Li cells at 0.5 C, **e** rate performance of a S/TiO_2/3DOMC/Li and S/3DOMC/Li cells at various current densities

the 2.0 V peak is due to the reduction of polysulfide to insoluble Li_2S_2 and eventually to Li_2S [25–28]. On the anodic scan, a peak at about 2.5 V is observed, which is associated with the oxidation of Li_2S_2/Li_2S to Li_2S_n, and from Li_2S_n to elemental S [29].

The discharging-charging curves of the S/TiO_2/3DOMC and S/3DOMC cathodes at a rate of 0.5 C (1 C = 1675 mA g^{-1}) are displayed in Fig. 8b and c, respectively. In Fig. 8b, the discharge capacities of S/TiO_2/3DOMC in the first three cycles were found to be 1105, 1002, and 897 mAh g^{-1}, respectively, and the discharging-charging platform corresponding to Fig. 8a could also be found. The discharge capacities of S/3DOMC cathode in the first three cycles were 902, 796, and 753 mAh g^{-1}, respectively, which is much lower than that of S/TiO_2/3DOMC. Figure 8d shows that both of the S/TiO_2/3DOMC and S/3DOMC cathodes exhibit good cycling stability over 150 cycles. However, as compared with that of S/3DOMC cathode, the S/TiO_2/3DOMC material shows obvious advantages in electrochemical capacity: it has a capacity of 1105 mAh g^{-1} in the initial cycle and a capacity of 695 mAh g^{-1} was maintained after 150 cycles, which equivalent to the discharge capacity decay of 0.24% per cycle. An overall coulombic efficiency of 98.6% was obtained after150 cycles, which demonstrates the excellent polysulfide retention capabilities of S/TiO_2/3DOMC material. It could be seen that, due to the strong adsorption between titanium dioxide and polysulfide, the addition of TiO_2 has significantly improved the performance of the batteries, both in terms of electrochemical capacity and cycle stability.

The S/TiO_2/3DOMC and S/3DOMC cathodes were further tested under different current densities (Fig. 8e). It can be seen that the S/TiO_2/3DOMC material has a distinct advantage over S/3DOMC in electrochemical performance. For the S/TiO_2/3DOMC cell, an initial discharge of 1074 mAh g^{-1} at 0.5 C was obtained, followed by relatively stable cycling at 857 mAh g^{-1}. As the current rate gradually rises to 1, 1.5, and 2 C, the reversible capacities of the S/TiO_2/3DOMC battery were also reduced to 782, 673, and 551 mAh g^{-1}, respectively. When the current rate came to 0.5 C again, the reversible specific capacity restored to about 792 mAh g^{-1}, which is very close to the original capacity. This observation is indicative for the cathode material's robustness and stability. Because of its three-dimensionally ordered macro/mesoporous structure, S/3DOMC cathode also has good sulfur loading ability with a good rate performance. However, the lack of strong adsorption of polysulfide by TiO_2 made it insufficient in terms of capacitance.

Conclusions

TiO_2/3DOMC composite was synthesized by a simple solvothermal synthesis and deposition process. The combination of several advantages of TiO_2/3DOMC including three-dimensionally ordered macro/mesoporous structure with a highly porous structure leads to a strong sulfur loading capacity and which could effectively inhibit polysulfides. Moreover, there is not only a good conductivity and structural restriction of carbon but an intense electrostatic attraction between metal-oxygen bond and polysulfides significantly of this material, which could improve the cycle performance of lithium/sulfur batteries. At 0.5 C, the initial discharge capacity reached 1105 mAh g^{-1} and the remaining capacity after 150 cycles was 695 mAh g^{-1}. Given the few jobs associated with carbon/TiO_2 applied to lithium-sulfur batteries, in this study, the nanostructural properties of the S/TiO_2/3DOMC composite and its electrochemical performance as a cathode for a lithium/sulfur battery were detected. Compared with some similar studies that have been done, for example, the novel CC/TiO_2/S composite prepared by Lei's group [17] and the Ti_4O_7-S cathodes made by Tao's team [18], having initial capacities of 1120 mAh g^{-1} and 1144 mAh g^{-1} in 0.2 C, respectively. Our research has found more possibilities for the application of carbon materials and titanium dioxide composites in cathode materials for lithium-sulfur batteries.

Funding information The study received financial support from the Program for the Outstanding Young Talents of Hebei Province; Scientific Research Foundation for Selected Overseas Chinese Scholars, Ministry of Human Resources and Social Security of China (Grant No. CG2015003002).

References

1. Marom R, Amalraj S, Leifer N, Jacob D, Aurbach D (2011) A review of advanced and practical lithium battery materials. J Mater Chem 21:9938–9954
2. Geng Z, Xiao Q, Wang D, Yi G, Xu Z, Li B, Zhang C (2016) Improved electrochemical performance of biomass-derived nanoporous carbon/sulfur composites cathode for lithium-sulfur batteries by nitrogen doping. Electrochim Acta 202:131–139
3. Lin Z, Liu Z, Fu W, Dudney N, Liang C (2013) Phosphorous pentasulfide as a novel additive for high-performance lithium-sulfur batteries. Adv Funct Mater 23:1064–1069
4. Manthiram A, Chung S, Zu C (2015) Lithium-sulfur batteries: progress and prospects. Adv Mater 27:1980–2006
5. Jeong Y, Lee K, Kim T, Kim J, Park J, Cho Y, Yang S, Park C (2016) Partially unzipped carbon nanotubes for high-rate and stable lithium–sulfur batteries. J Mater Chem A 4:819–826
6. He M, Yuan L, Zhang W, Hu X, Huang Y (2011) Enhanced cyclability for sulfur cathode achieved by a water-soluble binder. J Phys Chem C 115:15703–15709
7. Yang Y, Zheng G, Cui Y (2013) Nanostructured sulfur cathodes. Chem Soc Rev 42:3018–3032
8. Hou Y, Li J, Gao X, Wen Z, Yuan C, Chen J (2016) 3D dual-confined sulfur encapsulated in porous carbon nanosheets and wrapped with graphene aerogels as a cathode for advanced lithium sulfur batteries. Nanoscale 8:8228–8235

9. Zhang Z, Li Q, Jiang S, Zhang K, Lai Y, Li J (2015) Sulfur encapsulated in a TiO_2-anchored hollow carbon nanofiber hybrid nanostructure for lithium-sulfur batteries. Chem Eur J 21:1343–1349
10. Ji X, Lee K, Nazar L (2009) A highly ordered nanostructured carbon-sulphur cathode for lithium-sulphur batteries. Nat Mater 8: 500–506
11. Schuster J, He G, Mandlmeier B, Yim T, Lee K, Bein T, Nazar L (2012) Spherical ordered mesoporous carbon nanoparticles with high porosity for lithium–sulfur batteries. Angew Chem Int Ed 124:3591–3595
12. Xiao L, Cao Y, Xiao J, Schwenzer B, Engelhard M, Saraf L, Nie Z, Exarhos G, Liu J (2012) A soft approach to encapsulate sulfur: polyaniline nanotubes for lithium-sulfur batteries with long cycle life. Adv Mater 24:1176–1181
13. Wu B, Jiang X, Xiao L, Zhang W, Pan J, Ai X, Yang H, Cao Y (2014) Enhanced cycling stability of sulfur cathode surface-modified by poly(N-methylpyrrole). Electrochim Acta 135:108–113
14. Peng H, Zhang Q (2015) Designing host materials for sulfur cathodes: from physical confinement to surface chemistry. Angew Chem Int Ed 54:11018–110020
15. Chen X, Peng HJ, Zhang R, Hou TZ, Huang JQ, Li B, Zhang Q (2017) An analogous periodic law for strong anchoring of polysulfides on polar hosts in lithium sulfur batteries: S- or Li-binding on first-row transition-metal sulfides. ACS Energy Lett 2: 795–801
16. Yuan Z, Peng HJ, Hou TZ, Huang JQ, Chen CM, Wang DW, Cheng XB, Wei F, Zhang Q (2016) Powering lithium-sulphur battery performance by propelling polysulphide redox at sulphiphilic hosts. Nano Lett 16:519–527
17. Lei T, Xie Y, Wang X, Miao S, Xiong J, Yan C (2017) TiO_2 feather duster as effective polysulfides restrictor for enhanced electrochemical kinetics in lithium-sulfur batteries. Small 13:1701013
18. Tao X, Wang J, Ying Z, Cai Q, Zheng G, Gan Y, Huang H, Xia Y, Liang C, Zhang W, Cui Y (2014) Strong sulfur binding with conducting magnéli-phase Ti_nO_{2n-1} nanomaterials for improving lithium-sulfur batteries. Nano Lett 14:5288–5294
19. Li J, G J, Deng J, Huang Y (2017) Enhanced electrochemical performance of lithium-sulfur batteries by using mesoporous TiO_2 spheres as host materials for sulfur impregnation. Mater Lett 189: 188–191
20. Chen T, Cheng B, Zhu G, Chen R, Hu Y, Ma L et al (2017) Highly efficient retention of polysulfides in "sea urchin"-like carbon nanotube/nanopolyhedra superstructures as cathode material for ultralong-life lithium–sulfur batteries. Nano Lett 17:437–444
21. Chen T, Ma L, Cheng B, Chen R, Yi H, Zhu G, Wang Y, Liang J, Tie Z, Liu J, Jin Z (2017) Metallic and polar Co_9S_8 inlaid carbon hollow nanopolyhedra as efficient polysulfide mediator for lithium-sulfur batteries. Nano Energy 38:239–248
22. Chen T, Zhang Z, Cheng B et al (2017) Self-templated formation of interlaced carbon nanotubes threaded hollow Co_3S_4 nanoboxes for high-rate and heat-resistant lithium-sulfur batteries. J Am Chem Soc 139:12710–12715
23. Ma L, Zhang W, Wang L, Hu Y, Zhu G, Wang Y, Chen R, Chen T, Tie Z, Liu J, Jin Z (2018) Strong capillarity, chemisorption and electrocatalytic capability of crisscrossed nanostraws enabled flexible, high-rate and long-cycling lithium-sulfur batteries. ACS Nano 12:4868–4876
24. Ma L, Chen R, Zhu G, Hu Y, Wang Y, Chen T, Liu J, Jin Z (2017) Cerium oxide nanocrystal embedded bimodal micro-mesoporous nitrogen-rich carbon nanospheres as effective sulfur host for lithium-sulfur batteries. ACS Nano 11:7274–7283
25. Wang J, Wu Y, Shi Z, Wu C (2014) Mesoporous carbon with large pore volume and high surface area prepared by a co-assembling route for lithium-sulfur batteries. Electrochim Acta 144:307–314
26. Wang Z, Zhang S, Zhang L, Lin R, Wu X, Fang H, Ren Y (2014) Hollow spherical carbonized polypyrrole/sulfur composite cathode materials for lithium/sulfur cells with long cycle life. J Power Sources 248:337–342
27. Zhou G, Wang D, Li F, Hou P, Yin L, Liu C, Lu G, Gentlec I, Cheng H (2012) A flexible nanostructured Sulphur-carbon nanotube cathode with high rate performance for Li-S batteries. Energy Environ Sci 5:8901–8906
28. Zhang J, Yan X, Zhang J, Cai W, Wu Z, Zhang Z (2012) Preparation and electrochemical performance of TiO_2/C composite nanotubes as anode materials of lithium-ion batteries. J Power Sources 198: 223–228
29. Xiao Z, Yang Z, Wang L, Nie H, Zhong M, Lai Q, Xu X, Zhang L, Huang S (2015) A lightweight TiO_2/graphene interlayer, applied as a highly effective polysulfide absorbent for fast long-life lithium-sulfur batteries. Adv Mater 27:2891–2898